Conformational Fluctuation of Native-Like and Molten-Globule-Like Cytochrome c Observed by Time-Resolved Hole Burning[†]

Yutaka Shibata,*[,‡] Hirokazu Takahashi, Rina Kaneko, Atusi Kurita, and Takashi Kushida[§]

Department of Physics, Faculty of Science, Osaka University, Toyonaka, Osaka 560-0043, Japan

Received July 1, 1998; Revised Manuscript Received October 20, 1998

ABSTRACT: Nanosecond to millisecond conformational fluctuations of Zn-substituted cytochrome c (ZnCytc) have been studied by the time-resolved transient hole-burning method. The investigation of low-temperature dynamics has been made on the ZnCytc solution sample in a water−glycerol mixture. The conformational fluctuations in the native-like and the molten-globule (MG)-like states have been compared for the aqueous solution samples at room temperature. ZnCytc in the MG-like state has been prepared by adding 200 mM $NaClO_4$ to the protein solution with a pH of 2.1, and the formation of the MG-like state has been confirmed by both the far-UV CD and the visible absorption spectra. The hole spectrum of ZnCytc has been found to consist of two nearly degenerate components, that is, the Q_x and Q_y bands. The temporal change in the Q_x component hole spectrum has been extracted by fitting the observed hole spectrum to the three-Gaussian form. The experimental results for ZnCytc dissolved in a water−glycerol mixture have revealed that the conformational fluctuation of ZnCytc is suppressed around 200 K, which is nearly the same temperature as the glass-like transition point of Zn-substituted myoglobin (ZnMb) and also as the glass-transition point of the solvent. This supports the idea of the solvent-induced glass-like transition of a protein. It has been also found that at physiological temperatures the time scale of the conformational fluctuation of ZnCytc lies around a few tens of nanoseconds, which is 2−3 orders of magnitude faster than that of ZnMb. The experimental results for the aqueous solution samples have shown that the difference between the native-like and the MG-like states is not conspicuous. However, they are indicative of the appearance of the slower conformational fluctuation in the MG-like state.

In recent years, the conformational flexibility of a protein has received growing attention because of its great importance for protein functioning (*1*, *2*). Various experimental studies have given evidence for the conformational fluctuation of proteins (*3*−*6*). However, although the spatial aspect of such fluctuations has been clarified relatively well, the time scale in which such conformational fluctuations occur has not been clarified yet, because the observable in most cases is a time-averaged quantity. In fact, there have been only a few measurements that directly give the temporal aspect of the conformational fluctuation of a protein. This aspect is complementary to the spatial aspect and indispensable for obtaining a molecular-level understanding of biological processes of proteins. Thus, we emphasize here the particular importance of the time-domain observation of the conformational fluctuation of a protein.

Recently, we have succeeded in making a time-domain observation of the equilibrium conformational fluctuation of Zn-substituted myoglobin (ZnMb)[1] in the nanosecond to millisecond time region by using a novel method of time-resolved transient hole-burning (TRTHB) spectroscopy (*7*−*9*). In this technique, the temporal variation of the transient hole-burning spectrum burned by irradiation of a laser pulse is observed as a probe of the conformational fluctuation of a protein. The hole is formed while the excited chromophores are accumulated in the triplet state. Consequently, the lifetime of the hole corresponds to that of the triplet state which is usually in the millisecond time region. Owing to this long lifetime of the hole, this technique enables us to observe the conformational fluctuation in a very wide time region from nanoseconds up to milliseconds, and to estimate the equilibration time of the conformational fluctuation of a protein, which has not been available so far. To increase the internal conversion efficiency, we have replaced the heme in the intact protein by its Zn derivative. This metal substitution is also important experimentally to reduce the homogeneous width of the absorption spectrum, which is usually very broad in the case of the heme.

In this article, we apply this TRTHB technique to Zn-substituted cytochrome c (Zn-Cytc), which is a slightly smaller globular protein than Mb, and concerns the electrontransfer process in mitochondria. A compressibility study has suggested that Cytc is a somewhat more rigid protein than Mb, probably because of its lower content of α-helix, which is considered to induce incomplete packing within a

[†] This work was supported by the Research Fellowships of the Japan Society for the Promotion of Science for Young Scientists.

* To whom correspondence should be addressed.

[‡] Present address: Institute for Laser Technology, c/o Kansai Electric Power Company, 3-11-20, Nakoji, Amagasaki, Hyogo 661-0974, Japan.

[§] Present address: Graduate School of Materials Science, Nara Institute of Science and Technology, Ikoma, Nara 630-0101, Japan.

[1] Abbreviations: Cytc, cytochrome c; Mb, myoglobin; THB, transient hole burning; YAG, yttrium-aluminum-garnet; CW, continuous wave; CS's, conformational substates; MG, molten globule; UV, ultraviolet; CD, circular dichroism; OD, optical density; T-T, triplet−triplet; NMR, nuclear magnetic resonance.

10.1021/bi981568b CCC: $18.00
Published on Web 01/22/1999

protein molecule (*4*). Here, we are interested in how this difference is reflected on the results of the TRTHB measurement. We discuss the difference in the conformational dynamics between ZnCytc and ZnMb in terms of their structural and functional differences.

It has been also known that Cytc exhibits a transition from unfolded to molten−globule (MG) states by the addition of salt in an acidic condition (*10*−*14*). There has been a considerable interest in the MG state of a protein, which is considered to be a candidate for the intermediate state of the folding and unfolding processes of a protein (*15*−*17*). The conformation of a protein molecule in the MG state is believed to be more mobile than in the native state. On the basis of the experimentally observed similarity between the folding intermediate and the salt-induced MG state, a tentative scenario of the protein folding has been introduced as follows. In the course of folding, a protein molecule forms at first a folded state like a MG state in which the conformation of a protein fluctuates among many different and rather compact conformations. Then, in the next stage, the protein searches the unique and correct arrangement corresponding to the native conformation. This second stage, that is, the search of the native conformation among the MG-like conformations, is considered to be the rate-determining step of the folding.

Various kinetic investigations have indicated that the real folding process is not so simple as mentioned above (*18*, *19*). Here, nevertheless, we point out that, if the conformation of the folding intermediate is really similar to that of a protein in the salt-induced MG state, the search for the native conformation among the MG-like intermediate conformations is closely related to the fluctuation process in the static salt-induced MG state. Then, the equilibration time of the conformational fluctuation of a protein in the static MG state may give a rough measure of the search time for the native conformation among the transient MG-like conformers. Although the conformational fluctuation of a protein in the MG state has been characterized by various techniques (*14*, *20*−*22*), the time scale of the fluctuation has not been clarified so far. To estimate the equilibration time of the fluctuation process in the MG state as well as in the native state, we have prepared ZnCytc samples in the native-like state and in the MG-like state, and compared the dynamical features of these samples observed by the TRTHB technique.

EXPERIMENTAL PROCEDURES

(A) Materials. Horse cytochrome c (Type VI) was purchased from Sigma. ZnCytc was prepared according to the method of Vanderkooi et al. (*23*, *24*). First, metal-free Cytc (H_2Cytc) was obtained by reaction with anhydrous hydrofluoride, and it was purified by gel filtration through a column of Sephadex G-50. Then, $ZnCl_2$ was added to the solution at the lowered pH of 2.6 in a 10-fold molar excess over H_2Cytc. After the reaction for one hour at 50 °C and dialysis to appropriate buffer solutions, ZnCytc solution at a neutral pH was obtained.

For the neutral-pH samples, 50 mM ammonium acetate buffer of pH 5.0 was used. In the present work, a ZnCytc sample in the MG-like state was obtained by the addition of $NaClO_4$ at a low pH of ∼2.1. We lowered the pH of the sample solution by the addition of 0.1 N HCl up to an appropriate concentration to the neutral solution samples. The pH of the solution was monitored with a pH meter (Horiba, F-13). We took precaution not to lower the pH below 2 because lowering pH below 2 seems to dissociate the Zn atom irreversibly from the porphyrin molecule and result in the absorption spectrum characteristic of the porphyrin dication (PH_2^+). The typical HCl concentration was about 15 mM. For the TRTHB measurement on the MG-like ZnCytc in which the protein concentration is relatively high, it was necessary to suppress the $NaClO_4$ concentration below 200 mM to avoid aggregation of proteins. It was found that this $NaClO_4$ concentration is enough to stabilize the MG-like state of ZnCytc, as well as that of H_2Cytc (*25*). The protein concentrations in neutral buffer solutions were determined by using the previously reported molar extinction coefficients of $\epsilon_{416} = 129\ mM^{-1}\ cm^{-1}$ for FeCytc and $\epsilon_{423} = 243\ mM^{-1}\ cm^{-1}$ for ZnCytc (*24*). The protein concentration of the acidic solutions was estimated using that determined before adding HCl and by considering the volume change by the addition of HCl.

For the low-temperature TRTHB experiment, we mixed ZnCytc solution in the ammonium acetate buffer with a 3-fold volume of glycerol (ZnCytc-W:3G) to avoid cold denaturation of the protein and to maintain the sample transparent and clear even well below the ice point.

(B) Methods. Far-UV CD measurements were carried out by using a Jasco spectropolarimeter, Model J-720W. The protein concentration was about 0.1 mg/mL (∼8 μM), and a quartz cell with an optical path length of 1 mm was used.

In the low-temperature TRTHB experiment, the sample solution was sealed in a glass cell with an optical path length of 2 mm, and contained in a N_2-gas flow-type cryostat. The protein concentration was about 0.3 mM. The temperature was monitored by a thermocouple and maintained within ±0.5 K accuracy during the experiment. The sample solution remained transparent in the whole examined temperature region of 180−300 K.

In the case of MG-like ZnCytc in an aqueous solution, we could not prepare the sample with a high protein concentration because of the protein aggregation. We set the protein concentration at 0.08 mM for the MG-like sample and also for the control sample of the native-like ZnCytc in an aqueous solution. To achieve a sufficient optical density for these aqueous solution samples, we contained them in a cell with an optical path length of 10 mm. It was found that ZnCytc in the MG-like state is much less stable to the light irradiation than that in the native-like state. Therefore, the MG-like sample was kept stirred mildly by a magnetic stirrer in the experiment to prevent the sample from being damaged by the laser irradiation. The temperature of these aqueous solution samples was controlled by a Peltier device attached to one side of the cell.

The experimental setup of the TRTHB measurement is the same as that described in previous papers (*8*, *9*). The spectral hole was burned in the low-energy tail of the $Q(0, 0)$ absorption band around 580 nm by light pulses from a dye laser (Lambda Physik SCANMATE rhodamine B) pumped by a nanosecond-pulse Nd:YAG laser (Spectra Physics GCR-130). The pulse duration was about 7 ns, and the repetition rate was 10 Hz. Spontaneous emission from a dye solution (rhodamine 110 in ethanol, 0.2 g/L) pumped by another nanosecond laser (Spectra Physics TFR) was used

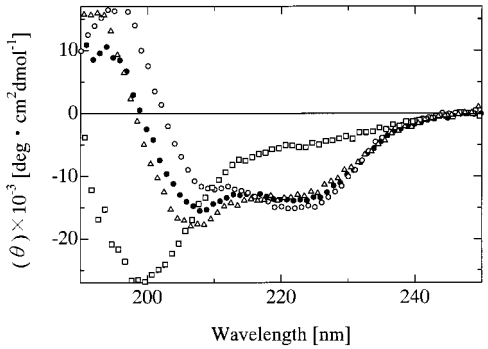

FIGURE 1: Room-temperature far-UV CD spectra of FeCytc at pH 5.0 with low salt concentration (○), ZnCytc at pH 5.0 with low salt concentration (●), at pH 2.0 with low salt concentration (□), and at pH 2.0 at 1 M $NaClO_4$ (△).

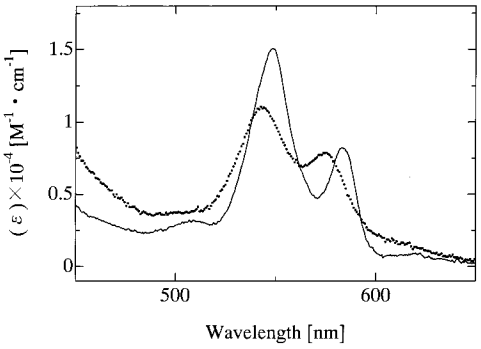

FIGURE 2: Room-temperature absorption spectra in the *Q* band region of ZnCytc at pH 7.0 with low salt concentration (solid line) and at pH 2.0 with 1 M $NaClO_4$ (dotted line). ϵ is the molar extinction coefficient.

for the probe light. The transmission light through the sample was analyzed through a 25 cm single-grating polychromator (Oriel MS257), and detected with a CCD camera system (Photometrics AT200) cooled by liquid nitrogen. The spectral resolution of the system was ~2 Å. The wavelength calibration of the polychromator system was done by using the 632.8 nm line of a He-Ne laser and the sharp lines of Hg atoms sealed in a fluorescent lamp at 546.1, 579.1, and 577.0 nm.

RESULTS AND ANALYSIS

(A) Spectroscopic Characterization of ZnCyt. The conformational state of the intact Cytc (FeCytc) has been well-studied as a function of temperature, pH, and the salt concentration. It is well-known that the addition of salt to FeCytc solution at a low pH level stabilizes the MG state of this protein (*10*−*13*, *20*, *22*, *26*). The conformational states of some metal-substituted Cytc's have also been investigated (*25*, *27*). On the basis of both the NMR and optical absorbance data, Anni et al. suggested that ZnCytc in a physiological condition has a similar tertiary structure to that of the native FeCytc. They gave evidence that His 18 and Met 80 offer the axial ligands to the Zn atom as in the case of native FeCytc. Contrary to this, it has been shown by Hamada et al. that H_2Cytc, which is known to lack the axial ligation of the porphyrin, assumes a MG-like conformation even in a physiological condition. Despite these investigations, the structural characteristics of ZnCytc at a low pH and a high-salt concentration have not been revealed yet. In order to make up for this deficiency, we measured the far-UV CD and visible absorption spectra of ZnCytc at pH values and salt concentrations relevant to our experiment.

Figure 1 shows the far-UV CD spectra of FeCytc at pH 5.0 with a low-salt concentration (FeCytc-N, ○), ZnCytc at pH 5.0 with a low-salt concentration (ZnCytc-N ●), at pH 2.0 with a low-salt concentration (ZnCytc-U, □), and at pH 2.0 and at 1 M $NaClO_4$ (ZnCytc-MG, △). The CD spectrum for FeCytc-N is the same as that in the literature (see, for example, ref *13*). It is found that the CD spectrum for ZnCytc-N is almost the same as that for FeCytc-N which shows minimums at 208 and 222 nm, although a slight deviation is observed between these spectra in the high-energy region. Thus, the results of the far-UV CD measurements support the conclusion drawn by Anni et al. that ZnCytc assumes almost the same conformation as that of FeCytc in a physiological condition (*27*).

Table 1: Absorption Maximum of Zn-Porphyrin Derivatives in Various Conditions

sample condition	Q(1, 0) band [nm]	Q(0, 0) band [nm]
ZnCytc−N	549	584
ZnCytc−MG	543	575
ZnMP−toluene[a]	532	569
ZnMP−pyridine[a]	543	578

[a] Reference *27*.

By contrast, the CD spectrum for ZnCytc-U has only one minimum around 200 nm, indicating the lack of the secondary structure, which is similar to the case of FeCytc in the unfolded state at low pH (see, for example, ref *13*). The spectrum for ZnCytc-MG has a shape similar to that of ZnCytc-N with two minimums at 208 and 222 nm, although a slight deviation is observed around 205 nm. This result is considered to imply the stabilization of the folded state by the addition of salt. This refolding induced by the salt addition is similar to that observed in FeCytc and H_2Cytc (*25*), and may be associated with the formation of the MG-like state under this condition. We also examined the effect of the addition of NaCl on the CD spectrum of ZnCytc at a lowm pH (data not shown). NaCl is known to be less effective for the formation of the MG state of FeCytc and H_2Cytc than $NaClO_4$ (*13*, *25*). It was found out that the addition of NaCl to ZnCytc solution at pH 2.0 hardly changes the CD spectrum up to the NaCl concentration of ~0.3 M, although this salt addition increases the negative value of the ellipticity at 222 nm above 0.3 M NaCl. This behavior is quite similar to that of H_2Cytc, but is different from that of FeCytc which refolds much more readily by the addition of NaCl. Thus, we can say that refolding of ZnCyt at a low pH requires a similar NaCl concentration to the case of H_2-Cytc, but a much higher NaCl concentration than the case of FeCytc. Possibly, this is reflective of a less effective coordination to the Zn atom in the porphyrin than that to the Fe atom in the heme.

In Figure 2, we show that the optical absorption spectra in the *Q* band region of ZnCytc-N (solid line) and ZnCytc-MG (dotted line). It is obvious that the absorption spectrum shows substantial variation according to the change in the solvent condition. It has been established that the absorption profile of Zn-porphyrin is sensitive to the ligation state of the Zn atom (*27*, *28*). We summarize in Table 1 the peak positions of the *Q* bands for ZnCytc under various conditions, as well as those for Zn mesoporphyrin in toluene and in

pyridine as typical examples of those without axial ligation and in the five-coordinate state, respectively. The absorption profile of ZnCytc-N is consistent with that obtained by Anni et al., indicating that ZnCytc-N is in the native-like state in which the Zn atom is in the six-coordinate state as the Fe atom in the native-state FeCytc (*27*). The results in Table 1 indicate that the absorption profile of ZnCytc-MG is characteristic of the five-coordinate Zn atom. This five-coordinate state of the Zn atom is consistent with the case of the MG-state FeCytc, in which the native ligand bond of Met 80 to the Fe atom is severed (*10*, *13*, *20*). It is necessary to make further experimental studies to clarify which residue(s) is (are) coordinated to the Zn atom in ZnCytc in this condition. Anyway, we can say from both the far-UV CD and absorption measurements that ZnCytc-MG is in the MG-like state, although it is still ambiguous whether its conformational state is the same as that of the MG-state FeCytc.

In the low-temperature experiment, we employed the sample of ZnCytc dissolved in a water−glycerol mixture with the volume ratio of 1:3 (ZnCytc−W:3G). It was found that ZnCytc−W:3G has almost the same absorption spectrum as that of ZnCytc-N, and that its absorption spectrum exhibits no substantial change by lowering temperature, except for a slight sharpening. Therefore, we consider that the ZnCytc molecule maintains the native-like structure even in a water−glycerol mixture and at low temperatures.

(B) Low-Temperature Dynamics of ZnCytc−W:3G. In ZnCytc, it is more difficult to detect the temporal variation of the THB spectrum than in the case of ZnMb because of the double peak characteristic of the $Q(0, 0)$ band of ZnCytc. It is well-known that the $Q(0, 0)$ band of Zn-porphyrin consists of almost degenerate two bands, that is, the so-called Q_x and Q_y components (*29*). In the case of ZnMb, these two bands fortunately split into two distinct bands probably because of the symmetry breaking by the environment, and then the temporal variation of the hole can be easily detected. Contrary to this, the Q_x and Q_y bands of ZnCytc are nearly degenerate, which makes it difficult to detect the temporal variation of the hole. We indicated in a previous paper (*30*) that the Q_x and Q_y components of the THB spectrum of ZnCytc can be distinguished at 180 and 200 K by analyzing the dependence of the THB spectrum on the polarization of the probe and burning beams. Since this analysis is based on the fact that the transition diples of these transitions cross at right angle, it is not possible to apply this analysis to the higher-temperature region where the rotational diffusion of the protein molecule also affects the polarization dependence of the THB spectrum. Figure 3b denotes the Q_x (dotted lines) and Q_y (dashed lines) components of the THB spectrum of ZnCytc−W:3G at 180 K obtained by the analysis of the polarization dependence. By convention, here we have labeled the transition component lower in energy as Q_x, and that higher in energy as Q_y. Figure 3a shows the absorption spectra before ($A(\omega)$, the dashed line) and after ($A'(\omega)$, the solid line) the burning. The total hole shape (solid line) in panel (b) corresponds to the difference spectra between A' and A in panel (a). The spike around the burning wavenumber in the spectra comes from the scattering of the burning laser light. It is obvious that both components of Q_x and Q_y give substantial contribution to the total hole shape. In the analysis of the observed TRTHB data for ZnCytc, therefore, one must consider this situation that complicates the experimental results.

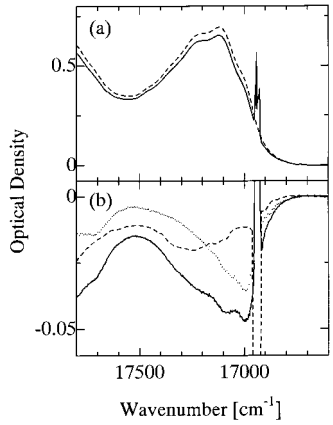

FIGURE 3: (a) Absorption spectra of ZnCytc−W:3G at 180 K before (dashed line) and after (solid line) the burning. (b) The total THB spectrum corresponding to the difference between the absorption spectra in (a) (solid line). The dotted and dashed lines are, respectively, the Q_x and Q_y component THB spectra, derived on the basis of the analysis of the polarization dependence of the hole spectra.

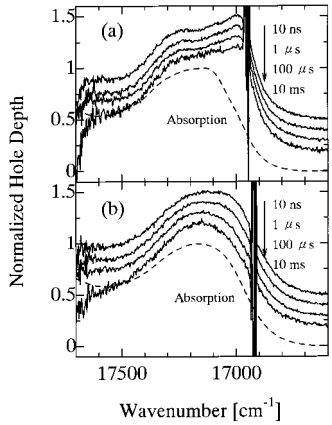

FIGURE 4: Time evolution of the normalized TRTHB spectra of ZnCytc−W:3G at 180 K (a) and 240 K (b). The spectra are offset vertically to avoid overlap. The dashed lines denote the normalized absorption spectra. The excitation wavenumber is 16 949 cm^{-1} for (a) and 16 920 cm^{-1} for (b).

Figure 4 shows the time evolution of the THB spectra of ZnCytc−W:3G (solid lines) at 180 K (panel a) and 240 K (panel b) for the delay time from 10 ns to 10 ms. We also show the ordinary absorption spectra (dashed lines) obtained at the same temperatures. Both the depth of the THB spectra and the height of the absorption spectra are normalized to unity for comparison. In Figure 4a, no apparent temporal variation is observed, suggesting that the conformational motion of ZnCytc is frozen out at 180 K. By contrast, Figure 4b clearly displays the temporal variation of the THB spectra at 240 K occurring in a characteristic manner of this sample. In the earlier stage of $t_d \leq 1$ μs, the hole spectrum has a broad profile implying its double-band characteristic, while in the later delay time region, its profile becomes sharper because of the relative decrease in the low-energy side. Anyway, it can be said from Figure 4b that the hole profile becomes similar to the absorption spectrum with prolonged delay time, suggesting that this time evolution reflects the conformational fluctuation of the protein. The temporal change in the THB spectrum in this case occurs so as to

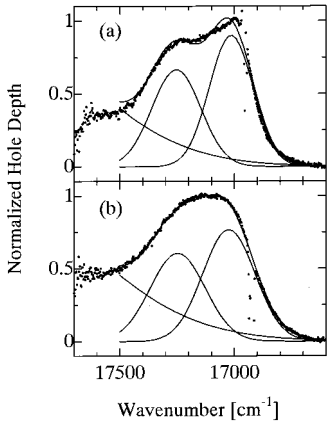

FIGURE 5: Normalized THB spectra (scattered dots) with the delay time of 10 ns at 180 K (a) and at 240 K (b) and the least mean-square fitting to the three-Gaussian profiles (solid lines).

narrow the splitting between the Q_x and Q_y bands, resulting in the loss of the low-energy side with prolonged delay time.

To make the temporal change in the hole spectra clearer, we fitted both the normalized hole and absorption spectra to a sum of three Gaussian functions,

$$H(\omega) = \sum_{i=x,y,\upsilon} \frac{A_i}{\sqrt{2\pi\sigma_i^2}} \exp\left[-\frac{(\omega-\omega_i)^2}{2\sigma_i^2}\right], \quad \text{with } \omega_x < \omega_y < \omega_\upsilon \quad (1)$$

These functions with $i = x$, y, and υ denote the Q_x, Q_y components of the $Q(0, 0)$ band, and the $Q(1, 0)$ band components, respectively. The last term, the contribution from the vibronic band, is necessary to fit the sloping baseline of the spectra due to the low-energy tail of this band. The peak position of the $Q(1, 0)$ band was found to be located at $\sim$18200 cm^{-1} at all temperatures examined. Therefore, we fixed ω_υ at 18200 cm^{-1} at all temperatures in the fitting of both the hole and absorption spectra. Further, we assumed that the relative area of the Q_y to Q_x band, A_y/A_x, is also temperature-independent. We estimated the value of A_y/A_x as 0.84 at 180 K and 0.82 at 200 K, by integrating the experimentally obtained Q_x and Q_y spectra over the wavenumber range of 16500−17500 cm^{-1}. Then, we fitted the observed spectra to eq 1 by the least mean square method with A_y/A_x constrained at the average value 0.83 over the wavenumber range of 16500−17500 cm^{-1}. We eliminated the distortions due to the laser scattering in the observed THB spectra by replacing the spectrum around the laser wavenumber with an appropriate quadratic function.

Figure 5 displays the results of the fitting. The data observed at low temperatures are in relatively poor agreement with the simulated curves, because the vibronic structure in the spectrum emerges in this temperature region. Above 200 K, all the observed spectra are well-fitted to the calculated one over the whole fitting wavenumber range. Figure 6 shows the time evolution of the calculated Q_x component hole spectrum (solid lines) together with the simulated Q_x component absorption spectrum (dashed line) at 240 K. The simulated hole spectrum clearly shows a temporal shift toward the peak position of the calculated absorption spectrum. The hole shift amounts to $\sim$20 cm^{-1}, which is far smaller than that previously observed for ZnMb (*8*, *9*). The

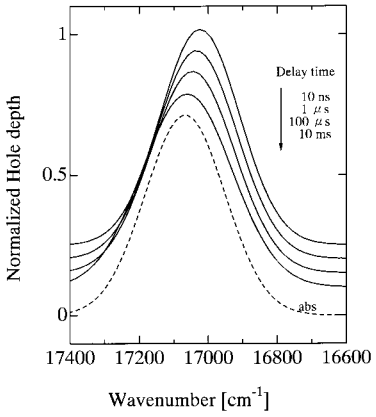

FIGURE 6: Time evolution of the simulated curve of the Q_x component hole spectrum at 240 K obtained by the three-Gaussian fitting. The dashed line denotes the simulated Q_x component absorption spectrum.

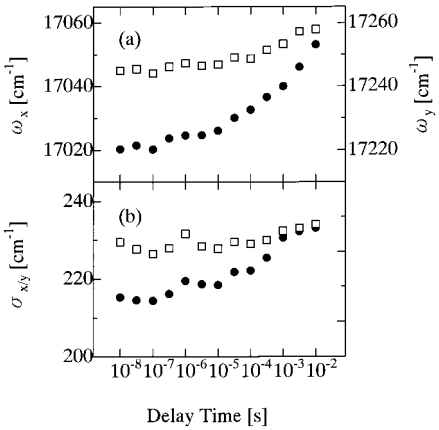

FIGURE 7: Time evolution of the peak energy of the Q_x and Q_y components, ω_x (●) and ω_y (□) (a), and that of the width, σ_x (f) and σ_y (□) (b), for ZnCytc−W:3G at 220 K.

temporal increase of the width also occurs in the simulated spectra, although it is not clear in Figure 6.

Figure 7 shows the typical time evolution of the peak positions (upper panel) and the widths (lower panel) of the Q_x (ω_x) and Q_y (ω_y) bands at 220 K estimated by the above fitting procedure. As a whole, the temporal variations of these four parameters occur in the same temporal region, suggesting that the temporal variation of the Q_x and Q_y component THB spectra is induced by the same conformational fluctuation. This tendency was observed in the whole temperature region examined. It is obvious in Figure 7 that the temporal changes in both the peak position and the width of the THB spectrum are larger for Q_x component than for Q_y component. This is probably because the electronic state of the Q_x excited state is more sensitive to the conformational change in the protein than that of the Q_y excited state. There is another plausible explanation for the smaller temporal change in the Q_y component THB spectrum: since the conformational selection by the laser excitation is done in the Q_x band, the selection in the Q_y band may not be as effective as in the Q_x band because of a distribution of the splitting between the Q_x and the Q_y bands. This initial incomplete selection results in a broader Q_y component THB spectrum just after the burning, and then makes the Q_y component THB spectrum less sensitive to the conformational fluctuation. This explanation is consistent with the observation in Figure 7 that the

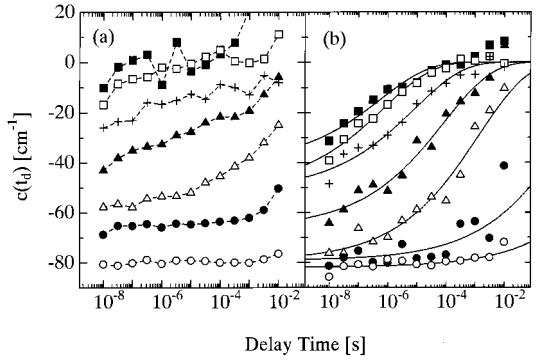

FIGURE 8: Time evolution of $c(t_d)$ for ZnCytc−W:3G (a) and ZnMb−W:3G (b) at 180 K (○), 200 K (●), 220 K (△), 240 K (▲), 260 K (+), 280 (K) (□), and 300 K (■). The data points at the same temperature in panel (a) are linked each other by dashed lines for guides of eyes. The solid lines in panel (b) are the fitting curves to the stretched exponential form.

initial hole width is larger for the Q_y component than for the Q_x component. Anyway, the most sensitive observable to the conformational fluctuation is the peak position of the Q_x component THB spectrum. Therefore, in the following analysis, we only consider the temporal variation of the peak energy ω_x of the Q_x component.

For further analysis of the temporal change in the THB spectra, we introduce a function $c(t_d)$ defined as

$$c(t_d) \equiv \omega_{x,\mathrm{THB}}(t_d) - \omega_{x,\mathrm{abs}} \qquad (2)$$

where $\omega_{x,\mathrm{THB}}(t_d)$ and $\omega_{x,\mathrm{abs}}$ are the center wavenumbers of the Q_x component Gaussian of the THB spectrum at the delay time of t_d and that of the absorption spectrum, respectively. When the deformed conformational distribution of the chromoprotein by the burning relaxes to the equilibrium distribution, the shape of the THB spectrum is expected to agree with that of the absorption spectrum. Then, in the limit of $t_d \rightarrow \infty$, $c(t_d)$ should tend to 0. In the limit of $t_d \rightarrow 0$, on the other hand, $c(t_d)$ will have a negative value, because the hole is formed initially in the low-energy tail of the absorption spectrum where the burning is made. In Figure 8a, we plot $c(t_d)$ for ZnCytc−W:3G at various temperatures as a function of t_d. The temporal change in $c(t_d)$ in the millisecond time region is not reliable because in this time region the chromophores accumulated in the triplet state begin to relax to the ground state and this hole-filling process may affect the hole shape. Except for this time region, $c(t_d)$ below ∼200 K remains at the initial negative value regardless of the increase of t_d, suggesting that the conformational fluctuation is suppressed in this temperature region. This suppression will be due to the so-called glass-like transition by lowering temperature, which has been observed for various proteins (*5*, *6*, *31*). At the intermediate temperatures, $c(t_d)$ shows a temporal change whose time scale becomes faster with increasing temperature. At and above 280 K, $c(t_d)$ again becomes almost t_d independent and has a value around 0, indicating that the conformational fluctuation is too fast to be detectable within the experimental time window.

In Figure 8b, we also show $c(t_d)$ for ZnMb dissolved in the same solvent as ZnCytc−W:3G (ZnMb−W:3G) obtained at various temperatures (*8*). We have already indicated that the effect of the Zn substitution to the secondary structure of Mb is negligible (*8*), and also that ZnMb can be regarded as in the native-like state. Since the overlap between the Q_x and Q_y bands is not significant in the case of ZnMb−W:3G (*30*), such analysis as was discussed above is not necessary. Accordingly, we defined $c(t_d)$ for ZnMb−W:3G simply as the time-dependent difference of the first moment between the THB and absorption spectra (*7*−*9*). In Figure 8b, the solid lines are the fitting curves to the stretched exponential function ($\exp[-(t_d/\tau)^{\beta}]$) with $\beta = 0.26$. Figure 8 shows clear difference in $c(t_d)$ between ZnCytc−W:3G and ZnMb−W:3G. At room temperature, the fluctuation-induced temporal variation in $c(t_d)$ for ZnCytc−W:3G seems to be completed within ∼100 ns, while that for ZnMb−W:3G lasts far longer, up to at least a few tens of microsecond. To our knowledge, this is the first time-domain measurement in which apparently protein-dependent dynamics has been observed. This also implies that the observed conformational dynamics is functionally important, and underscores the utility of the present TRTHB method. At 180 K, on the other hand, the t_d dependence of $c(t_d)$ is similar for both proteins, which is indicative of the glass-like transition.

(C) Dynamics of ZnCytc−N and ZnCytc−MG at Physiological Temperatures. Probably because we did not made any procedure to purge out the oxygen molecule which is a strong quencher of the triplet state, the lifetimes of the THB spectrum for the aqueous solution samples were ∼100 μs, which is much shorter than that in ZnCytc−W:3G. At present, it is not clear why the triplet lifetime is shortened only for the aqueous solution samples but not for the water−glycerol mixture sample. Perhaps quenching of the triplet state by the oxygen molecule is more effective in an aqueous solution than in a water−glycerol mixture. Because of this shortening of the hole lifetime, the time window of the TRTHB measurement is narrowed down to 10 ns−100 μs in the aqueous solution samples. Although this narrowing of the experimental time window prevents us from onbserving the slower stage of the fluctuation, the temporal variation of the observed hole spectrum is still considered to reflect the conformational dynamics of the protein correctly. This is because the temporal variation of the THB spectrum reflects the conformational fluctuation of the unexcited protein, and then it is not affected by the quenching of the triplet state.

Figure 9 shows the time evolution of the normalized THB spectra at 303 K for ZnCytc−N (panel a) and for ZnCytc−MG (panel b) together with the normalized absorption spectra. For both cases, the THB spectra appear to display no apparent temporal variation. This is because the time scale of the conformational fluctuation is very fast as compared with the experimental time scale in this temperature region. Nevertheless, a detailed experiment showed that the hole profile actually varies with time, especially in the earliest stage of $t_d \leq 100$ ns. For both samples, the temporal variation of the hole shape occurs as the decrease in its low-energy side, which is similar to the case of ZnCytc−W:3G. As a clearer measure of the temporal variation of the THB spectra, here we again introduce $c(t_d)$ defined by eq 2. To obtain $c(t_d)$ for ZnCytc−N, the observed THB spectra were fitted to the three-Gaussian form of eq 1, with the same assumptions of $\omega_v = 18200$ cm^{-1} and $A_y/A_x = 0.83$ as those used in the fitting of the THB spectra for ZnCytc−W:3G. All of the observed data were well-fitted to this three-Gaussian expression.

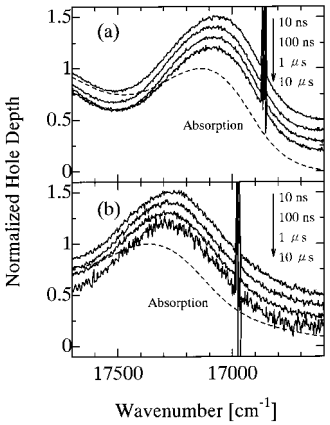

FIGURE 9: Time evolution of the normalized TRTHB spectra of ZnCytc−N (a) and ZnCytc−MG (b) at 303 K. The spectra are offset vertically to avoid overlap. The dashed lines denote the normalized absorption spectra. The excitation wavenumber is 16 863 cm^{-1} for (a) and 16 978 cm^{-1} for (b).

In the case of ZnCytc−MG, on the other hand, this definition for $c(t_d)$ does not seem to be reasonable, because ZnCytc−MG has the absorption spectrum around 578 nm that is characteristic of a five-coordinate Zn-porphyrin. In Zn porphyrin of this state, the Q_x and Q_y component spectra have not been identified yet, and therefore, the assumption of $A_y/A_x = 0.83$ is no longer valid in this case. Hence, we have no basis to fit the observed hole spectra for ZnCytc−MG to eq 1. In fact, the observed spectra could not be fitted adequately to eq 1 with a tentative assumption of $A_y/A_x = 0.83$. Accordingly, we define $c(t_d)$ for ZnCytc−MG in a way similar to that for the ZnMb sample (*8*) as the time-dependent difference of the first moment between the THB and absorption spectra,

$$c(t_d) \equiv \frac{\int_{\omega_1}^{\omega_2} \omega H(\omega, t_d)\mathrm{d}\omega}{\int_{\omega_1}^{\omega_2} H(\omega, t_d)\mathrm{d}\omega} - \frac{\int_{\omega_1}^{\omega_2} \omega A(\omega)\mathrm{d}\omega}{\int_{\omega_1}^{\omega_2} A(\omega)\mathrm{d}\omega} \qquad (3)$$

Here, ω_1 and ω_2 are the low- and high-energy limits of the calculation, respectively. As pointed out above, the THB spectra for ZnCytc−MG exhibit the temporal variation mainly as the decrease in the low-energy side of the spectra. Therefore, we carried out the integration in eq 3 within the low-energy side of the spectra. We defined the low- (ω_1) and high- (ω_2) energy limits of the calculation as the spectral positions in the low-energy side where the height of the spectrum is 20% and 80% of its maximum, respectively. On determination of ω_1 and ω_2, the observed spectra were smoothed by averaging beforehand. Then, the numerical integration in eq 3 was made for the spectra before smoothing, in which we again eliminated the distortions due to the laser scattering by replacing the spectrum around the laser wavenumber to an appropriate quadratic function. Tentatively, we calculated $c(t_d)$ for ZnCytc−N according to eq 3 as well as according to eq 2, and confirmed that $c(t_d)$'s calculated according to both expressions reproduce almost the same temporal behavior. Thus, we interpret that the employment of eq 3 instead of eq 2 does not cause a serious problem.

In Figure 10, we compare the time evolution of $c(t_d)$ obtained at 283, 293, and 303 K between ZnCytc−N (panel a) and ZnCytc−MG (panel b). Now, it becomes evident that the temporal change in the THB spectra actually occurs for both samples especially in the earliest stage. Stepwise changes in $c(t_d)$ are seen at $t_d = 100$ μs for both samples, probably because the hole-filling process around 100 μs time region deforms the hole shape. For comparison, we also plot $c(t_d)$ obtained for ZnMb in an aqueous solution at 280 and 300 K in panel (a), in which the temporal change continues up to a far slower time region. $c(t_d)$ for ZnCytc−N does not reach 0 even in the time region where its temporal change appears to be completed. This is against our expectation that the hole profile becomes equal to the absorption profile and then $c(t_d)$ becomes 0 when the distorted energy distribution of the chromophore by the burning recovers the equilibrium distribution. This discrepancy is explained as follows. In the spectrum A', the increase of OD is also observed owing to the transition of the accumulated molecules in the triplet state into the higher triplet state, as well as the decrease of OD due to the depletion of the molecules in the ground state. If the former component due to the triplet-triplet (T-T) transition overlaps the spectral region of the THB spectrum, it deforms the THB spectrum and then becomes a serious obstacle for the measurement. In most cases of Zn-porphyrin derivatives, however, it has been known that the T-T spectrum lies on the high-energy side of the *Q* band and the overlap between this and the *Q*-band spectrum is not serious (*32*, *33*). In the case of ZnCyt−N, the low-energy tail of the T-T spectrum may overlap the THB spectrum and cause a sloping baseline in the THB spectrum. Then, $c(t_d)$ does not reach 0 even well after its temporal change is completed. Considering this situation, we infer from Figure 10 that the temporal change in $c(t_d)$ for the native-like ZnCytc is completed within 100 ns. This time scale is consistent with the results for ZnCytc−W:3G, and is much faster as compared with the cases of ZnMb in an aqueous solution.

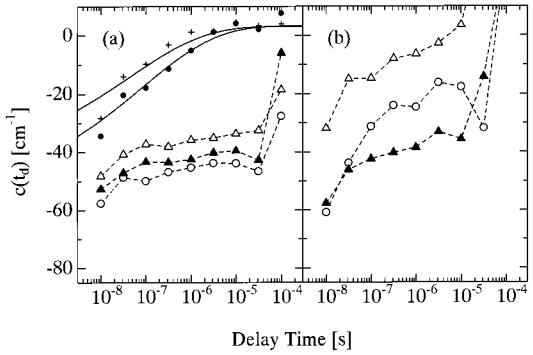

FIGURE 10: Time evolution of $c(t_d)$ for ZnCytc−N (a) and ZnCytc−MG (b) at 283 K (○), 293 K (▲), and 303 K (△). The data for ZnMb in an aqueous solution at 280 K (●) and 300 K (+) are also shown in panel (a). The data points at the same temperature are linked to each other by dashed lines for guides of eyes. The solid lines in panel (a) are the fitting curves of the data for ZnMb to the stretched exponential form.

Seemingly, the time evolution of $c(t_d)$ for ZnCytc−MG is similar to that for ZnCytc−N as a whole. However, a detailed inspection of Figure 10 discloses some different tendencies in $c(t_d)$ between the native-like and MG-like samples. That is, $c(t_d)$ for ZnCytc−MG appears to display a temporal change in two phases, consisting of the primary steep change until ~100 ns and the following long-time tail from 100 ns up to 10 μs or longer. Because of the unfortunate

shortening of the hole lifetime, it is not obvious whether the slower phase of the fluctuation process for ZnCytc−MG is completed within the experimental time window. An experiment on the sample with a sufficiently long lifetime of the triplet state is necessary to clarify the long-time behavior of the THB spectrum for ZnCytc−MG. Anyway, this difference may be a possible sign of the different dynamical characteristics between the native-like and MG-like ZnCytc.

DISCUSSION

(A) Comparison between ZnCytc and ZnMb. So far, the fluctuation of the protein conformation has been investigated by various experimental techniques (*3*, *5*). Among these investigations, the compressibility study has offered the most systematic information about the conformational fluctuation of proteins (*4*, *22*, *34*, *35*). In the compressibility study, several volumetric properties, such as the partial compressibility or the partial volume fluctuation of a protein molecule, are used as a measure of its conformational flexibility. It has been pointed out that cavities in the interior of a protein give a predominant contribution to its partial volume fluctuation, and that such cavities originate mainly from the incomplete packing of the hydrophobic residues or in the interface between the α-helices. Accordingly, a protein molecule having a high α-helical content is inferred to have a large fluctuation of the partial volume. Gekko et al. have estimated that the partial volume fluctuation of cytochrome c is 30.8 mL/mol, while that of myoglobin, which is known to be a typical α-helix protein, is 64.1 mL/mol (*4*).

This different flexibility between Cytc and Mb suggested by the compressibility study appears to be reflected clearly on the results of the present TRTHB experiments. In Figures 8 and 10a, we have compared the time evolution of $c(t_d)$ associated with the equilibrium conformational fluctuation of proteins between the presently studied ZnCytc and the previously studied ZnMb. Here, we compare the dynamics of ZnCytc and ZnMb only in the native-like state. The most conspicuous difference in the temporal behavior of $c(t_d)$ between these samples is that the temporal change for ZnMb continues up to a much slower time region than that for the native-like ZnCytc, especially at high temperatures. In addition, the temporal change in $c(t_d)$ for ZnMb seems to occur in a wider time region than that for the native-like ZnCytc, although this tendency is not clear in the intermediate temperature region of 220−240 K. These two tendencies may directly reflect the different dynamical characteristics between ZnCytc and ZnMb.

From the comparison between ZnCytc and ZnMb mentioned above, it is supposed that the more flexible characteristic of Mb probably due to its larger α-helical content results in a slower conformational fluctuation. Inversely, this leads to a tentative interpretation that the slower stage of the temporal change in $c(t_d)$ around the microsecond time region seen only in ZnMb originates from the slow rearrangement motion of the hydrophobic residues or of the packing topology in the interface between the α-helices. We also interpret that ZnCytc containing a smaller amount of α-helices possesses a smaller amount of slow conformational motions, and then lacks the slower stage of the temporal change in $c(t_d)$ in the microsecond time region.

We consider that the above-mentioned difference in the dynamical characteristics of ZnCytc and ZnMb may be relevant to their functional difference. Cytc is known to be concerned with the electron-transfer process in mitochondria, which is almost a pure electronic process and seems to need no large internal displacement of atoms. On the other hand, in a Mb molecule which functions as a container of oxygen molecules in a muscle cell, a relatively large displacement of atoms is considered to be necessary for entry and release of an oxygen molecule (*36*, *37*). Hence, it may be suggested that the temporal change in $c(t_d)$ of ZnMb in the later stage of 100 ns−10 μs, which is absent in the native-like ZnCytc, has a close relationship to the entry and release of the oxygen molecule. Indeed, as reported in a previous paper, the time scale of the ligand escape entrance process of the intact Mb shows a temperature dependence similar to that for the time scale of the temporal change in $c(t_d)$ for ZnMb (*8*). To confirm this relation, one needs further systematic measurements.

In the low-temperature region, $c(t_d)$ for both protein samples showed a similar tendency as shown in Figure 8 in spite of the distinct behavior at higher temperatures. Namely, they become almost time-independent below ∼200 K, implying the suppression of the conformational fluctuation in this temperature region. In a previous paper (*8*) and an accompanying paper (*9*), we claimed the validity of the idea that the quenching of the conformational dynamics of protein by lowering temperature is caused by the freezing of the surrounding solvent (*38*, *39*). The present observation indicates that the glass-like transition of the proteins having rather different conformational flexibility set in at almost the same temperature corresponding to the vitrification temperature of the solvent. This again supports the idea of the solvent-induced glass-like transition of protein.

(B) Comparison between Native-Like and MG-Like ZnCytc. Various experimental studies have verified that proteins in the MG state have a more flexible conformation than those in the native state (*11*−*14*). Recently, by using the compressibility study, Chalikian et al. have compared the volumetric properties of Cytc among the native state, the acid-induced unfolded state, and the salt-induced MG state (*22*). They have indicated that the partial volume fluctuation of Cytc amounts to ∼0.6% and ∼2.0% of its average partial volume in the native state and in the salt-induced MG state, respectively. This result suggests a much more mobile conformation of the protein in the MG state. It has been inferred that this larger conformational fluctuation of FeCytc in the MG state than in the native state comes from the increase in the volume of the hydrophobic core accompanied by the native-to-MG transition (*12*, *20*).

Although it is not so evident, the result of the present TRTHB measurement shown in Figure 10 suggests different dynamical characteristics of ZnCyt in the native-like and MG-like states. Whereas the temporal change in $c(t_d)$ for ZnCytc−N occurs only in the early stage of $t_d \leq 100$ ns, that for ZnCytc−MG seems to consist of two phases. One is a similar process to that for ZnCytc−N occurring within ∼100 ns, and the other is the long-time tail following the former phase and occurs over the time range from 100 ns up to 10 μs or longer. The appearance of the slower fluctuation phase in the MG-like state may be associated with its larger flexibility indicated by the volumetric study. As pointed out in the comparison between ZnCytc and ZnMb in the native-like state, here it is again suggested that larger

conformational fluctuations of a protein result in slower processes. We suppose that the slower phase in the temporal change in $c(t_d)$ appearing in the case of ZnCytc−MG is associated with the rearrangement of the residues in the hydrophobic core region which is considered to expand in the MG-like state.

The conformational equilibration time of a protein molecule in the static MG state has important meaning because it is an approximate measure of the time scale of the search for the native conformation from the transient MG-like state formed initially in the folding process. In the present study, however, although the appearance of a slower fluctuation in the MG-like state was observed, the equilibration time in the MG-like state could not be estimated because of the shortening of the triplet lifetime. The observation of the long-time behavior especially in the millisecond time region is necessary in order to discuss the relationship between the fluctuation process of the MG-like ZnCytc and the folding kinetics. A further investigation of the conformational state of ZnCytc−MG is also necessary.

ACKNOWLEDGMENT

The authors express their gratitude to Prof. Yuji Goto, Dr. Daizo Hamada, and Prof. Saburo Aimoto of Osaka University for their help in preparation of Zn-substituted cytochrome c and measurements of the CD spectra, and also for fruitful advice in characterization of the conformational state of ZnCytc in various conditions.

REFERENCES

1. Karplus, M., and McCammon, J. A. (1981) *CRC Crit. Rev. Biochem. 9*, 293−349.
2. Welch, G. R. (1986) in *The Fluctuating Enzyme*, Wiley Interscience, New York.
3. Frauenfelder, H., Petsko, G. A., and Tsernoglou, D. (1979) *Nature 280*, 558−563.
4. Gekko, K., and Hasegawa, Y. (1986) *Biochemistry 25*, 6563−6571.
5. Doster, W., Cusack, S., and Petry, W. (1989) *Nature 337*, 754−756.
6. Rasmussen, B. F., Stock, A. M., Ringe, D., and Petsko, A. (1992) *Nature 357*, 423−424.
7. Shibata, Y., Kurita, A., and Kushida, T. (1997) *J. Lumin. 72*−*74*, 605−606.
8. Shibata, Y., Kurita, A., and Kushida, T. (1998) *Biophys. J. 75*, 521−527.
9. Shibata, Y., Kurita, A., and Kushida, T. (1999) *Biochemistry 38*, 1789−1801.
10. Dyson, H. J., and Beattie, J. K. (1982) *J. Biol. Chem. 257*, 2267−2273.
11. Ohgushi, M., and Wada, A. (1983) *FEBS Lett. 164*, 21−24.
12. Goto, Y., Calciano, L. J., and Fink, A. L. (1990) *Proc. Natl. Acad. Sci. U.S.A. 87*, 573−577.
13. Goto, Y., Takahashi, N., and Fink, A. L. (1990) *Biochemistry 29*, 3480−3488.
14. Goto, Y., Hagihara, Y., Hamada, D., Hoshino, M., and Nishii, I. (1993) *Biochemistry 32*, 11878−11885.
15. Ptitsyn, O. B. (1987) *J. Protein Chem. 6*, 273−293.
16. Kuwajima, K. (1989) *Proteins 6*, 87−103.
17. Elöve, G. A., Chaffotte, A. F., Roder, H., and Goldberg, M. E. (1992) *Biochemistry 31*, 6876−6883.
18. Takahashi, S., Yeh, S. R., Das, T. K., Chan, C. K., Gottfried, D. S., and Rousseau, D. L. (1997) *Nat. Struct. Biol. 4*, 44−50.
19. Yeh, S. R., Takahashi, S., Fan, B., and Rousseau, D. L. (1997) *Nat. Struct. Biol. 4*, 51−56.
20. Jeng, M. F., Englander, S. W., Elöve, G. A., Wand, A. J., and Roder, H. (1990) *Biochemistry 29*, 10433−10437.
21. Nolting, B., and Sligar, S. G. (1993) *Biochemistry 32*, 12319−12323.
22. Chalikian, T. V., Gindikin, V. S., and Breslauer, K. (1995) *J. Mol. Biol. 250*, 291−306.
23. Vanderkooi, J. M., and Erecinska, M. (1975) *Eur. J. Biochem. 60*, 199−207.
24. Vanderkooi, J. M., Adar, F., and Erecinska, M. (1976) *Eur. J. Biochem. 64*, 381−387.
25. Hamada, D., Kuroda, Y., Kataoka, M., Aimoto, S., Yoshimura, T., and Goto, Y. (1996) *J. Mol. Biol. 256*, 172−186.
26. Myer, Y. P., and Saturno, A. P. (1990) *J. Protein Chem. 9*, 379−387.
27. Anni, H., Vanderkooi, J. M., and Mayne, L. (1995) *Biochemistry 34*, 5744−5753.
28. Nappa, M., and Valentine, J. S. (1978) *J. Am. Chem. So. 100*, 5075−5080.
29. Gouterman, M. (1978) in *The Porphyrins* (Dolphin, D., Ed.) Vol. 3, pp 12−24, Academic Press, New York.
30. Shibata, Y., and Kushida, T. (1998) *Chem. Phys. Lett. 284*, 115−120.
31. Iben, I. E. T., Braunstein, D., Doster, W., Frauenfelder, H., Hong, M. K., Johnson, J. B., Luck, S., Ormos, P., Schulte, A., Steinbach, P. J., Xie, A. H., and Young, R. D. (1989) *Phys. Rev. Lett. 62*, 1916−1919.
32. Tsvirko, M. P., Sapunov, V. V., and Solovev, K. N. (1973) *Opt. Spectrosc. 34*, 635−638.
33. Shibata, Y. (1997) Ph.D. Thesis, Osaka University.
34. Iqbal, M., and Verrall, R. E. (1987) *J. Phys. Chem. 91*, 1935−1941.
35. Gekko, K., and Hasegawa, Y. (1989) *J. Phys. Chem. 93*, 426−429.
36. Case, D. A., and Karplus, M. (1979) *J. Mol. Biol. 132*, 343−368.
37. Tian, W. D., Sage, J. T., and Champion, P. M. (1993) *J. Mol. Biol. 233*, 155−166.
38. Mayer, E. (1994) *Biophys. J. 67*, 862−873.
39. Hagen, S. J., Hofrichter, J., and Eaton, W. A. (1995) *Science 269*, 959−962.

BI981568B